

Synthesis of Directly and Doubly Linked Dioxoisobacteriochlorin Dimers

Satoru Hiroto, Ichiro Hisaki, Hiroshi Shinokubo,^{†,*} and Atsuhiko Osuka*

Department of Chemistry, Graduate School of Science, Kyoto University, Sakyo-ku, Kyoto 606-8502, Japan

Received September 27, 2008; E-mail: hshino@apchem.nagoya-u.ac.jp; osuka@kuchem.kyoto-u.ac.jp

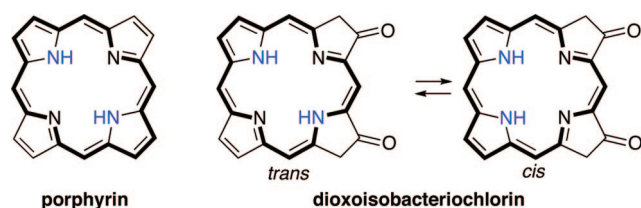
Porphyrin has a flexible π -electronic system that is sensitive to peripheral substituents. Among peripherally modified porphyrins, hydroxyporphyrin has been only scarcely studied so far, despite its analogy to phenols, which are key players in the benzenoid chemistry. Crossley et al. reported that keto–enol tautomerism of β -hydroxyporphyrins depends on solvent polarity.¹ This tautomerism has a large impact on the optical property of porphyrin, since the keto- and enol-forms correspond to a chlorin and a normal porphyrin, respectively.

In natural systems, isobacteriochlorins and dioxoisobacteriochlorin are important prosthetic groups found in dissimilatory nitrite reductase.² While extensive studies have been made toward these pigments,³ the isobacteriochlorin chromophore has been unexplored for *meso*-aryl porphyrins. Here we report the serendipitous synthesis and unique structure of doubly linked cofacial dioxoisobacteriochlorin dimers.

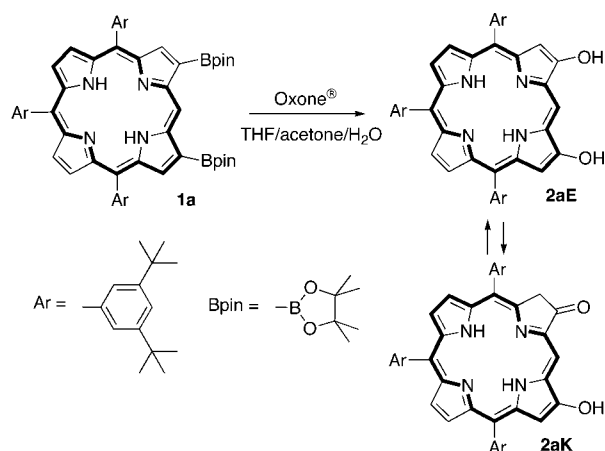
Recently, we reported a highly selective functionalization of porphyrins at β -positions by the iridium-catalyzed direct borylation.^{4,5} The oxidation of the boryl groups in **1a** with oxone (2KHSO₅·KHSO₄·K₂SO₄) afforded 2,18-dihydroxyporphyrin **2a** in 88% yield, which is a potential precursor for isobacteriochlorin, oxoisobacteriochlorin, or dioxoisobacteriochlorin, depending upon keto–enol tautomerism or change of the oxidation state (Scheme 1). In accord with the report by Crossley et al., **2a** shows keto–enol tautomerism depending on solvents: a keto–enol form **2aK** was predominant in CDCl₃, while a bis-enol-form **2aE** was exclusively detected in DMSO-*d*₆ (Supporting Information, Figure S1). Absorption and emission spectra of **2a** are also solvent-dependent (Figure S12). Interestingly, the keto–enol form **2aK** constructs a dimeric assembly with complementary intermolecular hydrogen bonding in its concentrated solution. The binding constant in CDCl₃ was determined to be 34 M⁻¹ by ¹H NMR titration (Figure S11).

We then attempted further oxidation of **2a** with DDQ with a hope to obtain a dioxoisobacteriochlorin (Scheme 2). To our surprise, however, we found the formation of a sole product **3a**, which exhibits its parent mass ion peak at $m/z = 1811.1469$ (calcd for (C₁₂₄H₁₄₅N₈O₄)⁺: $m/z = 1811.1416$ [(M + H)⁺] in its high-resolution electrospray-ionization time-of-flight (HR ESI-TOF) mass spectrum. The ¹H NMR spectrum of **3a** shows two pyrrole- β protons at 8.37 and 8.17 ppm, indicating a symmetric structure of **3a**. In addition, one singlet *sp*³ proton at 4.81 ppm suggests the presence of two carbonyl groups in **3a**. Importantly, one singlet meso proton appeared in a significantly shielded region at 5.59 ppm indicating its face-to-face dimeric structure. From these spectral features, we assigned **3a** to be a dimerized product of dioxoisobacteriochlorin.⁶ The use of PbO₂ as an oxidant improved the yield up to 47%. The similar oxidation of Ni(II) and Zn(II) porphyrins **2b** and **2c** provided the corresponding nickel and zinc complexes **3b** and **3c** in 48% yield and 18% yield, respectively. Zinc(II)

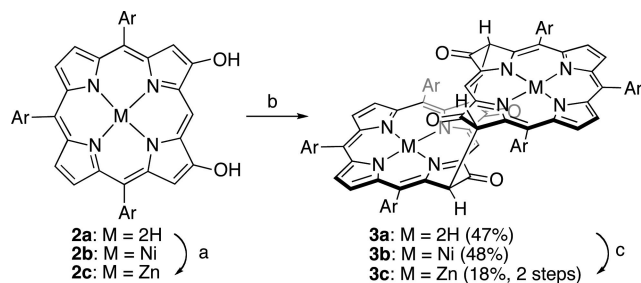
Chart 1



Scheme 1. Synthesis and Keto–Enol Tautomerism of **2a**



Scheme 2. Oxidation of **2a**



^a Conditions: (a) Zn(OAc)₂·2H₂O, CH₂Cl₂/MeOH, room temp, 1 h. (b) PbO₂, PhCF₃, 60 °C, 24 h for **2a** and **2c**; DDQ, CH₂Cl₂, room temp, 48 h for **2b**. (c) Zn(OAc)₂, NaOAc, CHCl₃, MeOH, reflux, 24 h, 48%.

complex **3c** can also be prepared by metalation of **3a** with Zn(OAc)₂·2H₂O in moderate yield. Interestingly, keto–enol tautomerism was not observed for **3**.

The structure of **3a** and **3b** were unambiguously confirmed by X-ray diffraction analysis (Figure 1, and Figure S14).⁷ The bond lengths between bridging β -carbons are 1.60 and 1.59 Å in **3a** and **3b**, respectively, which are slightly longer than a typical single bond. Their distorted structures were seemingly caused by π -electronic repulsion due to close location of isobacteriochlorin cores forced by such short linkages. The distance between two cores, which is defined as the distance between two mean planes composed of three

[†] Present address: Department of Applied Chemistry, Graduate School of Engineering, Nagoya University, Nagoya 464-8603, Japan.

carbon and two nitrogen atoms around the meso carbon of each core, are 3.32 Å for **3a** and 3.51 Å for **3b**.

Figure 2 shows UV–vis absorption spectra of **3a**, **3b**, and **3c** in dichloromethane. Free base **3a** shows splitting Soret bands at 425 and 485 nm and Q bands at 584, 631, and 674 nm. The splitting of the Soret band may be caused by exciton coupling between two closely located isobacteriochlorin units. In comparison to **3a**, the metal complexes **3b** and **3c** exhibit slight red-shifted and splitting Soret-like bands at 418 and 453 nm, and 450 and 469 nm, respectively. More interestingly, substantially red-shifted lowest Q bands are observed at 759 and 751 nm, respectively, indicating a significant change in the HOMO–LUMO gap induced by metalation.

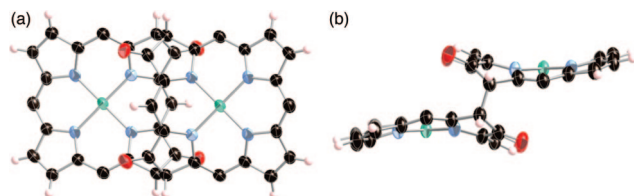


Figure 1. X-ray crystal structure of **3b**: (a) top view and (b) side view. Thermal ellipsoids are at 50% probability level. Meso substituents are omitted for clarity.

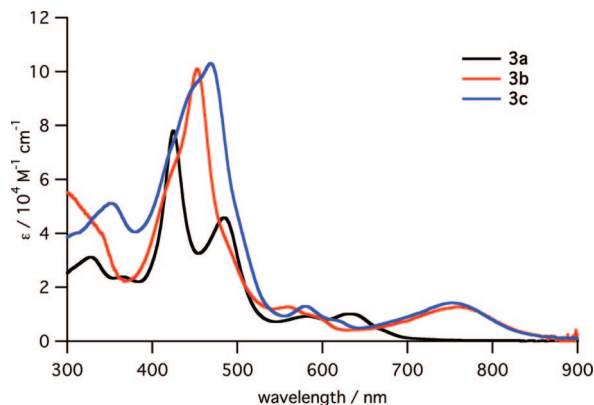


Figure 2. UV–vis absorption spectra of **3a**, **3b**, and **3c** in dichloromethane.

To investigate the intramolecular electronic interaction between two isobacteriochlorin moieties, cyclic voltammetry was performed in dichloromethane solution with Bu_4NPF_6 as electrolyte (Figure S16). For **3b**, two reversible oxidation potentials at 0.42 and 0.65 V and an irreversible reduction potential at -1.34 V were observed (vs ferrocene/ferrocenium). The splitting oxidation potentials indicate the existence of strong π -electronic intramolecular interactions of **3b**. Such splitting oxidation potentials were also observed for **3a** at 0.45 and 0.69 V, but the irreversible reduction potential was substantially lowered to -1.52 V. Thus, the HOMO–LUMO gaps were estimated for **3a**, **3b**, and **3c** to be 1.96, 1.77, and 1.65 V, respectively. This tendency is in good agreement with that observed in absorption spectra. To investigate the origin of the much larger HOMO–LUMO gap of **3a** than **3b** and **3c**, MO calculations were performed. Dioxoisobacteriochlorin has two cis and trans isomers along with NH tautomerism (Chart 1). Consequently,

geometry optimizations were performed for three different isomers, cis–cis, trans–cis, and trans–trans dimers, at the B3LYP/6–31G(d) level. Among these isomers, the cis–cis dimer has the smallest energy, indicating that this is the predominant structure for **3a**. The HOMO–LUMO gaps decrease as the order of cis–cis (2.53 eV), trans–cis (2.23 eV), and trans–trans (2.14 eV) (Figure S17). Compared to the HOMO–LUMO gap of **3b** (2.07 eV), the larger HOMO–LUMO gap of **3a** is accounted for by the cis–cis isomer of isobacteriochlorin freebase dimer. The cis–cis conformation is also supported by the diffraction analysis: the X-ray structure is better suited with the calculated cis–cis structure. Variable-temperature ^1H NMR analysis of **3a** from -90 to 25 °C in CD_2Cl_2 confirmed the presence of two species at lower temperatures, probably indicating NH tautomerization of **3a** (Figure S14).

In summary, we investigated solvent dependent keto–enol tautomerism of 2,18-dihydroxyporphyrins. Furthermore, we found unique reactivity of them to produce isobacteriochlorin dimers upon oxidation. This is the first example of directly linked isobacteriochlorin dimers, which will open up new chemistry of isobacteriochlorin as well as face-to-face porphyrin dimers. The plausible mechanism for the formation of **3** probably involves dimerization of quinone-like diketoporphyrin, which is generated by the oxidative dehydrogenation of **2** (Scheme S1). Further investigation on the quinone-like diketoporphyrin intermediate is currently under way in our laboratory.

Acknowledgment. This work was supported by Grant-in-Aids for Scientific Research (No. 18685013) from MEXT, Japan, and S.H. acknowledges the Research Fellowships of JSPS for Young Scientists.

Supporting Information Available: General procedures, spectral data for compounds, and CIF files. This material is available free of charge via the Internet at <http://pubs.acs.org>.

References

- Crossley, M. J.; Hardwig, M. M.; Sternhell, S. *J. Org. Chem.* **1988**, *53*, 1132 For a *meso*-hydroxyporphyrin, see: Esdaile, L. J.; Senge, M. O.; Arnold, D. P. *Chem. Commun.* **2006**, 4192.
- (a) Murphy, M. J.; Siegel, L. M.; Kamin, H.; Rosenthal, D. *J. Biol. Chem.* **1973**, *248*, 2801. (b) Chang, C. K. *J. Biol. Chem.* **1985**, *260*, 9520.
- (a) Scott, A. I.; Irwin, A. J.; Siegel, L. M.; Shooleerly, J. N. *J. Am. Chem. Soc.* **1978**, *100*, 7987. (a) Stolzenberg, A. M.; Spreer, L. O.; Holm, R. H. *J. Am. Chem. Soc.* **1980**, *102*, 364. (b) Wu, W.; Chang, C. K. *J. Am. Chem. Soc.* **1987**, *109*, 3148.
- Hata, H.; Shinokubo, H.; Osuka, A. *J. Am. Chem. Soc.* **2005**, *127*, 8264.
- (a) Yamaguchi, S.; Kato, T.; Shinokubo, H.; Osuka, A. *J. Am. Chem. Soc.* **2007**, *129*, 6392. (b) Hisaki, I.; Hiroto, H.; Shinokubo, H.; Osuka, A. *Angew. Chem., Int. Ed.* **2007**, *46*, 5125. (c) Song, J.; Jang, S. Y.; Yamaguchi, S.; Sanker, J.; Hiroto, S.; Aratani, N.; Shin, J.-Y.; Easwaramoorthi, S.; Kim, K. S.; Kim, D.; Shinokubo, H.; Osuka, A. *Angew. Chem., Int. Ed.* **2008**, *47*, 6007.
- For related dimerization of oxophlorins, see: (a) Fuhrop, J.-H.; Baumgartner, E.; Bauer, H. *J. Am. Chem. Soc.* **1981**, *103*, 5854. (b) Khoury, R. G.; Jaquinod, L.; Nurco, D. J.; Pandey, R. K.; Senge, M. O.; Smith, K. M. *Angew. Chem., Int. Ed. Engl.* **1996**, *35*, 2496.
- The crystallographic data of **3a**: $\text{C}_{127}\text{H}_{147}\text{N}_8\text{O}_4\text{Cl}_9$, $M = 2168.58$, triclinic, space group $P1$ (No. 2), $a = 14.333(2)$, $b = 16.550(3)$, $c = 27.977(5)$ Å, $\alpha = 93.212(3)$, $\beta = 103.856(3)$, $\gamma = 110.975(3)^\circ$, $V = 5942.3(17)$ Å³, $Z = 2$, $T = 90(2)$ K, $\rho_{\text{calcd}} = 1.212$ g/cm, $R_1 = 0.0937$ ($I > 2\sigma(I)$), $wR_2 = 0.3056$ (all data), GOF = 1.047. **3b**: $\text{C}_{127}\text{H}_{143}\text{N}_9\text{O}_4\text{Ni}_2\text{Cl}_4$, $M = 2110.96$, triclinic, space group $P1$ (No. 2), $a = 13.188(5)$, $b = 14.388(5)$, $c = 16.656(7)$ Å, $\alpha = 66.993(12)$, $\beta = 86.554(14)$, $\gamma = 78.472(12)^\circ$, $V = 2849.9(19)$ Å³, $Z = 1$, $T = 123$ K, $\rho_{\text{calcd}} = 1.230$ g/cm, $R_1 = 0.0860$ ($I > 2\sigma(I)$), $wR_2 = 0.2661$ (all data), GOF = 1.029.

JA807659H